LEAD-FREE LOW-MELTING-POINT GLASS AS BONDING AGENT FOR TiO_2 NANOPARTICLE COATINGS

S. Lopez-Esteban[*1], B. Cabal[2], A. Borrell[3], J.F. Bartolome[1], A. Fernandez[2], M. Faraldos[4], A. Bahamonde[4], J.S. Moya[2], C. Pecharroman[1]

[1]Instituto de Ciencia de Materiales de Madrid (ICMM-CSIC), C/ Sor Juana Ines de la Cruz, 3, Cantoblanco, 28049 Madrid (Spain)
[2]Centro de Investigacion en Nanomateriales y Nanotecnologia (CINN) (CSIC-UO-PA), Avenida de La Vega 4-6, 33940, El Entrego, Asturias (Spain)
[3] Instituto de Tecnologia de Materiales, Universitat Politecnica de Valencia, Camino de Vera S/N, 46022, Valencia (Spain)
[4] Instituto de Catalisis y Petroleoquimica (ICP-CSIC), C/ Marie Curie, 2, Cantoblanco, 28049, Madrid (Spain)

[*] Corresponding author: Dr. Sonia Lopez-Esteban.
E-mail address: s.lopez.esteban@csic.es
Instituto de Ciencia de Materiales de Madrid (ICMM)
Consejo Superior de Investigaciones Cientificas (CSIC)
Sor Juana Ines de la Cruz, 3
Cantoblanco, 28049 Madrid
Spain
Tel.: +34-91.334.90.00
Fax: +34-91.372.06.23

ABSTRACT

This work is a study of the properties of TiO_2-anatase nanoparticles attached by a low- melting point inorganic glass (530°C). Unlike other low-melting glasses, this composition does not contain any toxic metal. Likewise, it shows an excellent wettability on ceramic nanoparticles. A small addition of 5 vol.% of glass remarkably enhances the mechanical strength of the composites with respect to pure TiO_2 calcined at the same temperature, reaching the double value. Self-cleaning properties analyzed using the methylene blue 365 nm UV-A photodegradation test showed that, after different UV-light periods, the photo-efficiency of TiO_2-anatase was not altered by the presence of this glass.

Keywords

B. Nanoparticles, C. Photocatalysis, D. TiO_2, D. Glass.

1. INTRODUCTION

On one hand, titanium dioxide (TiO_2) is the world's main pigment to provide whiteness, brightness and opacity, and its use is widely spread in coatings and paints [1,2]. Secondly, titanium dioxide based photocatalysts are recognized by their acknowledged effectiveness on various chemical pollutants [3–6]. Finally, TiO_2 based photocatalysts have great potential for the inactivation of damaging pathogens, as successfully triggered the destruction of different viruses and bacteria [7–12].

It is known that the efficiency of the photocatalytic reactions of TiO_2 is increased when these particles have a nanometric size, since they expose more surface area per unit volume than in the case of micrometric particles. However, the use of nanoparticles is limited, first, by their tendency to agglomerate -hindering its homogeneous dispersion when incorporated as an additive in different systems- and, second, by its toxicity[13], to the point that they are considered carcinogenic to humans when inhaled[14]. Nanoparticles have shown a demonstrated toxicity in vertebrates, invertebrates, plants and algae, with the consequent risk to health and environmental impact[15]. By supporting them on a matrix, the agglomeration, the release to environment and the toxicity of the nanoparticles is avoided.

For the attachment of the nanoparticles to a surface, the presence of binder materials is essential and, generally, such binders have an organic nature (polymers). When titanium dioxide is exposed to light, it absorbs UV light, which initiates a chain of events that lead to the production of free radicals. These radicals can attack the surroundings of the pigment, which can cause the decomposition of the organic environment, resulting in fragility, loss of brightness, loosing of dust, etc. In the

particular case of paints, when pigments or dyes are involved, the color can also be affected, resulting in a yellowish color. Considering the crystallographic forms of TiO_2, anatase and rutile, these problems are less relevant in the case of rutile as, for pure phases, it is generally accepted that anatase exhibits a higher photocatalytic activity compared to rutile [16,17]. Thus, the use of organic binders forces the use of rutile instead of anatase, diminishing the photocatalytic activity of the product. In this sense, we propose the use of an inorganic glass as binder of the TiO_2 nanoparticles in order to be able to use anatase and maximize the photocatalytic activity of the coating.

The use of inorganic supports to achieve an isolated distribution of anatase nanoparticles has been investigated in devices where TiO_2 provides very favorable properties in microwave frequencies. This is the case of composites formed by anatase/low melting glass [18] for applications in the electronics sector. However, these glasses have lead in their composition, a material whose repeated exposure can have serious and irreversible effects on neurological behavior and development [19], particularly in children. This problem derived from the use of lead has headed the European Union to regulate the marketing and use of products that contain this element[20]. It is, therefore, a chemical element which should be avoided as much as possible.

In summary, in the present work we propose the use of a lead-free low melting point glass as bonding agent of the TiO_2-anatase nanoparticles which allows, through a wetting/spreading process, that the nanoparticles appear effectively dispersed and firmly attached. The mechanical properties of a set of sintered samples have been

studied, and their catalytic properties have been measured by the degradation of methylene blue under the application of ultraviolet light during different time periods.

2. EXPERIMENTAL

2.1 STARTING MATERIALS

A fine-particulate, pure titanium dioxide (*Aeroxide® TiO_2 P 25*, *Evonik Industries*) has been used. A low melting glass belonging to the P_2O_5-CaO-Na_2O system, which was developed by the authors in a previous investigation [21], with a composition of 45 mol% P_2O_5, 10 mol% CaO, 45 mol% Na_2O (45P 10C 45N) has been used. This glass was obtained by a melting process from the precursors ($NH_4H_2PO_4$, $CaCO_3$ and Na_2CO_3). The precursors were completely mixed in the proper proportion to the composition. The heat treatment was carried out in two stages in a 10% Pt/Rh crucible. In the first stage, the mixture of the precursors was treated at 350°C for 1 h to favor their decomposition. In the second stage, the resulting mixture was treated at 900°C for 1 h and suddenly cooled. The cooled glass frit was ground in agate mortar and sieved to obtain a particle size below 45 µm. In order to prepare the composites, the TiO_2 and glass powders were mixed in the proportions tested (1, 3, 5, 10, 20 vol.% glass) and passed through mortar until a homogeneous powder was obtained.

2.2 STRUCTURAL AND THERMAL CHARACTERIZATION

The X-ray diffraction analysis (XRD) was carried out using a Bruker D8 Advance diffractometer. The patterns were recorded over the angular range of 2°−60° (2θ) using Cu Kα radiation.

The textural characterization of pure TiO_2 and the TiO_2/5 vol.% glass composite was carried out by measuring the N_2 adsorption-desorption isotherms at -196ºC in an automatic apparatus (*Micromeritics* ASAP 2420). Before the experiments, the samples were outgassed under vacuum at 140ºC overnight. The isotherms were used to calculate specific surface area S_{BET}

The thermal behavior of the materials was studied by Environmental Scanning Electron Microscopy (ESEM) and Heating Microscopy: (i) The observations with the ESEM (*Philips XL30 ESEM*) were carried out by placing some grains of glass on the surface of a compacted TiO_2 piece (5 mm diameter, 2 mm thick) and subsequently heating from room temperature up to 700°C, with heating rates of 20°C/min. (ii) The heating microscope (HMS, *Hesse Instruments,* model HR18) was equipped with *Leica Microsystems* optics and EMI software (automated Image Analysis High temperature). The glass samples (10x14x2 mm) were placed on an alumina support and heated in air at the following rates: 80°C/min in the range 20°C-80°C, and 10°C/min in the range between 80°C and the flow point. The tests were made following the standard DIN 51730 (1998-4) / ISO 540 (1995-03-15), excluding sphere and flow temperature.

The microstructure of the heated specimens was studied by Field Emission Scanning Electron Microscopy (FE-SEM, *FEI Nova NANOSEM 230*) after machining and polishing down to 1 μm.

2.3 SAMPLES PREPARATION

In order to obtain discs, the powders were compressed in stainless steel dies with different diameters (20 mm for mechanical properties, 30 mm for catalysis tests), with

1 Ton uniaxial pressure. Subsequently, the discs were subjected to heating in oven at 10°C/min up to 530°C, maintained for 12 minutes to ensure uniformity, and quenched to room temperature out of the oven. The samples had slightly contracted after the process.

2.4 MECHANICAL CHARACTERIZATION

Fifteen specimens of each glass content in the range 1-20 vol.% glass, as well as pure titania for comparison purposes, were subjected to biaxial flexural strength tests in a universal testing machine (*Shimadzu Auto Graph AG-X5kN*, Japan). The biaxial flexural strength was measured using the piston-on-3-ball method (ISO 6872 standard). A disc of the material to be tested was placed on three balls separated by 120° on a 10 mm diameter circle. The tests were performed at room temperature at a crosshead speed of 1 mm/min. Samples with 18 mm diameter, and thickness in the range 1.7 mm-2 mm were used [22,23].

2.5 PHOTOCATALYTIC ACTIVITY

Catalysts with 27.5 mm diameter and 1.8 mm thickness were used for the photocatalytic study. Only the samples with low content were tested (1, 3 and 5 vol. % glass) as well as pure titania for comparison purposes. A spot of Methylene Blue (MB) was deposited on each substrate by spraying with a 0.8 mm nozzle airbrush (Defynik 140 by *Sagola*) operating at 3 bar air pressure, 5 mL of MB solution 5 x 10^{-4} M (2.5 micromoles) in acetone. The distance between nozzle and substrate (150 mm) and

volume/concentration of MB solution were previously optimized to obtain a homogeneous rounded spot with enough colour contrast.

The photocatalytic activity tests to evaluate the MB photodegradation were carried out in a metal chamber equipped with an ultraviolet LED emitting at 385 nm, located at the top of the chamber, that provided 34.70 $mW \cdot cm^{-2}$ measured on the surface of the specimens. The photocatalytic degradation of MB was followed by acquisition of UV-spectra of each specimen at different irradiation times (from minute fractions up to 2.6 hours) by UV-Vis diffuse reflectance (*Jasco V720* spectrophotometer). The obtained data were transformed into Kubelka-Munk units. For each time, the integrated relative intensity was determined and normalized with respect to the t=0 intensity.

3. RESULTS AND DISCUSSION

X-ray diffraction has been used for identification of phases. Figure 1 shows the XRD patterns of the commercial powder titania with 5 vol.% glass, before and after annealing at 530°C for 12 minutes ((a) and (b), respectively). The patterns for the other glass contents are completely analogous (data not shown), and they all match well with tetragonal anatase and rutile (Powder Diffraction Files Nos. 21-1272, 21-1276, International Centre for Diffraction Data (ICDD), respectively). Based on the intensity of the diffraction peaks (Figure 1), and according to the calculations found in the literature [16,17] all the composites studied contain a similar ratio $f_{anatasa}/f_{rutile}$ of 0.83/0.17 before annealing. This ratio changes to 0.78/0.22 after annealing up to 530°C and, therefore, at least 78 wt% TiO_2 is anatase. Annealing at this low temperature allows for the complete

crystallization of P25, for which amorphous TiO_2 transforms to anatase, while the amount of rutile remains constant. According to this result, we can state that the titania remains mainly in the crystallographic form of anatase. This was predictable, as anatase converts to rutile at temperatures ranging between 550°C and about 1000°C[16–18].

The presence of either or both of anatase and rutile affects the material's photocatalytic performance [24]**.** We propose for these materials the use of anatase instead of rutile, which increases the photocatalytic activity of the material. In this sense, there are clear advantages: I) In the case of paintings, the use of an inorganic glass instead of an organic vehicle avoids the degradation of the binder for the photocatalytic activity of the titania, preserving the properties of the material. II) As the disinfection capability of titanium dioxide is primarily attributed to surface generation of reactive oxygen species as well as free metal ions formation, its capacity is greatly increased by the use of anatase, with a better photocatalytic activity than rutile.

Figure 2 shows the images taken both by ESEM and Heating Microscopy at three different temperatures (20°C, 300°C and 550°C). According to the results of the Heating Microscope, the characteristic temperatures for this glass were found to be 416°C as deformation temperature and 563°C as flow temperature. According to the DTA results obtained in a previous work[21], the glass transition (Tg), crystallization temperatures (Tc) and melting temperature (Tm) for this glass were determined: Tg=325°C, Tc=435°C, Tm=530°C. As can be observed at Figure 2, at 300°C, as the temperature has not yet reached the deformation temperature (416°C), the image of ESEM has not much changed with respect to the one at room temperature, showing still sharp edges in the glass particles. However, at 550°C the temperature is over the deformation point, the

contact angles have decreased and the sharp edges have turned to become rounded. Finally, the contact angles at 563°C have decreased to 29° and 25° (left and right, respectively). This is an indication that this particular glass composition presents an excellent wettability on ceramic substrates, either titania (ESEM test) or alumina (HM test).

Concerning the mechanical properties, it has been found that the biaxial flexural strength of all the composites tested was superior to that of pure titania (Figure 3). Whereas the biaxial flexural strength measured for pure TiO_2 was close to 10 MPa, the resistance of the composites titania/glass reached the range 13-19 MPa. The highest result (19 MPa) was obtained for the samples with 5 vol. % glass, who nearly doubled the resistance obtained for pure titania. Thus**,** the glass improves extraordinarily the mechanical strength of pure TiO_2, as glass plays the role of a cement for titania nanoparticles. This glass offers the possibility of attaching firmly the titania nanoparticles as a cement and – due to its high wettability- a very low volume of glass is needed to avoid loose nanoparticles that could be inhaled, decreasing the toxicity and improving, therefore, the health security.

Figure 4A exhibits a FE-SEM image of the sample of TiO_2/glass with a high volume fraction of glass (20 vol% glass). It has been verified that, even at high glass contents, such glass is homogeneously dispersed on the TiO_2 matrix. Figure 4B shows a detail of the ceramic/glass interface, where can be observed that the glass presents a good wettability on the ceramic particles. Likewise, there is no evidence of reaction between components.

The degradation of methylene blue in all the composites studied is shown in Figure 5A. The resulting slope in all the curves was found to be the same, demonstrating that the photocatalytic capacity of TiO_2 has not been altered by the presence of glass. Likewise, the results of the BET surfaces measured under the same conditions were found to be similar (pure TiO_2: 35 m^2/g; TiO_2/5 vol.% glass composite: 30 m^2/g), the BET surface in the composites is reduced by only 15% with respect to that of pure TiO2, which warrants that the photocatalytic properties of TiO_2 are barely affected. Therefore, the incorporation of the low-melting point glass did not sacrifice available surface area of photocatalyst, and, in this sense, the expected catalytic properties of TiO_2 keep unaltered.

As mentioned above, along with its acknowledged effectiveness on various chemical pollutants, TiO_2 provides simultaneously disinfection and decontamination, which will certainly offer a potential alternative to conventional procedures as a promising candidate for the passive reduction of transmission of pathogen agents. For several decades, the application of titanium dioxide as an antimicrobial has been recognized and used for this purpose in manufactured materials as well as in air and water purification [25,26]. An advantage is that, eventually, the microbes and organics are mineralized to carbon dioxide and water. Another benefit is that titanium dioxide is not consumed in the process of photocatalysis. Because its action is believed to be primarily due to photocatalysis, it has been always seen as a benign, environmentally friendly means of destruction of both chemical and microbial contaminates. According to the results obtained in this work, the glass selected presents the advantage of be cured in situ with a heat treatment at low temperature (530°C). This circumstance allows considering that this TiO_2-anatase/glass composite could be potentially used as a coating

or paint of surfaces (walls, floors, ceramic tiles, doors, etc.) that need to be maintained clean and hygienic. Its use is also proposed as an additive in construction materials, such as tiles, bricks, cements, etc., in order to pursue the same aim.

One of the possible applications that we also propose is to print 3D structures [27–31] and functionalize them with heavy metals that have catalytic capacity, interesting especially for drug and phytosanitary synthesis. It is worth pointing out in water use the possibility of recovering the photocatalyst more easily because it can be dimensioned so as not to have to use ultrafiltration. One could even "paint" the surface of the reactor itself or an insert in it. Therefore, a wide spectrum of possible applications of immobilized photocatalyst opens up, which avoids the costs of reusing it.

In summary, the use of a small volume fraction (1-5 vol. %) of this lead-free low-melting-point glass as an inorganic additive allows to use mainly anatase. By using an inorganic component, the degradation observed in conventional paints is avoided. In the TiO_2-anatase/glass compacts, titanium dioxide maintains its many advantages including low cost, chemical stability, non-toxicity, and ability to use ultraviolet light energy (300–400 nm) for taking advantage of its excellent photocatalytic activity. Regarding the lead-free glass, it offers an extraordinary relevance with respect to health and environment. Its low-melting point allows the coating or paint to be cured *in situ* with a heat treatment at low temperature. Moreover, it increases the mechanical resistance of the composites up to twice.

4. CONCLUSIONS

The incorporation of the low-melting point glass involves annealing at low temperature, which allows the titania to remain mainly in the crystallographic form of anatase, that exhibits superior catalytic properties than rutile. Such incorporation keeps the catalytic properties of TiO_2 unaltered. The glass presents a good wettability on the ceramic surfaces and does not contain toxic metals, which means that can be considered environmental friendly. It has been showed that the glass improves remarkably the mechanical properties of the composites with respect to pure TiO_2 by a factor of up to 2, as glass plays the role of a cement for titania nanoparticles. It avoids loose nanoparticles that could be inhaled, decreasing the toxicity for loosen nanoparticles and improving, therefore, the security for the health.

ACKNOWLEDGEMENTS

This work was supported by CSIC under grant 201960E103. Dr. Borrell acknowledges the Spanish Ministry of Economy and Competitiveness for her RyC contract (RYC-2016-20915).

FIGURE CAPTIONS

Figure 1. X-Ray diffractograms corresponding to sample TiO_2/5 vol.% glass, (a) before annealing up to 530°C and (b) after annealing.

Figure 2. Environmental Scanning Electron Microscope (ESEM) images taken at three different temperatures: A) 20°C, B) 300°C, C) 550°C. The inserts show the Heating Microscope images corresponding to each temperature.

Figure 3. Biaxial flexural strength of samples with different glass content.

Figure 4. FE-SEM micrographs corresponding to a sintered sample TiO_2/20 vol% glass. In micrograph (B), the upper area corresponds to TiO_2 and the lower area corresponds to glass.

Figure 5. (A) Comparison of the evolution of the degradation of methylene blue projected on pure TiO_2, and on composites of TiO_2 with 1, 3 and 5 vol.% glass, respectively. (B) Degradation of methylene blue on the disc of the TiO_2/5vol.% glass composite, under exposure to 380 nm ultraviolet radiation.

FIGURES

FIGURE 1

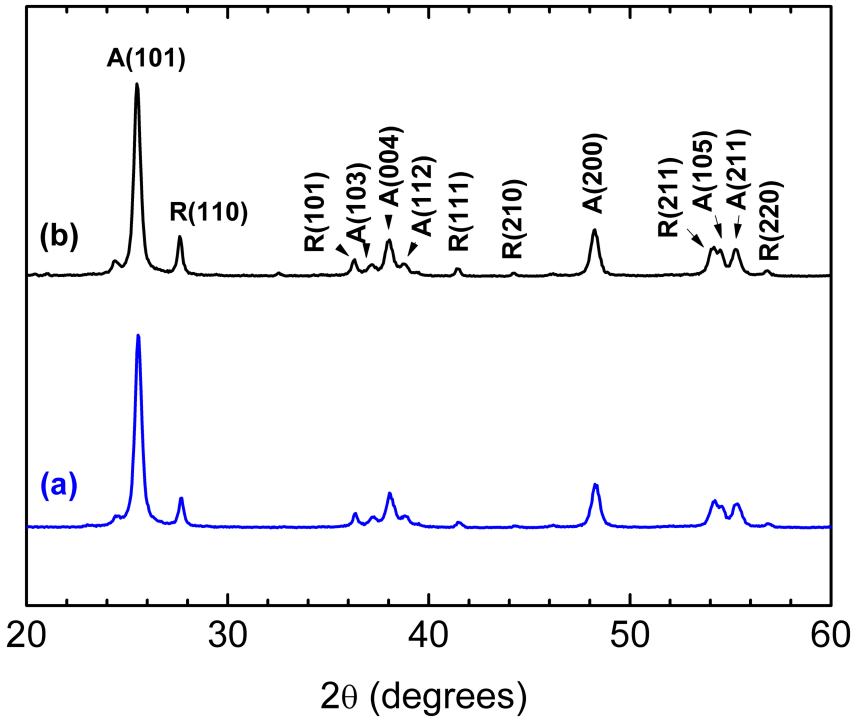

FIGURE 2

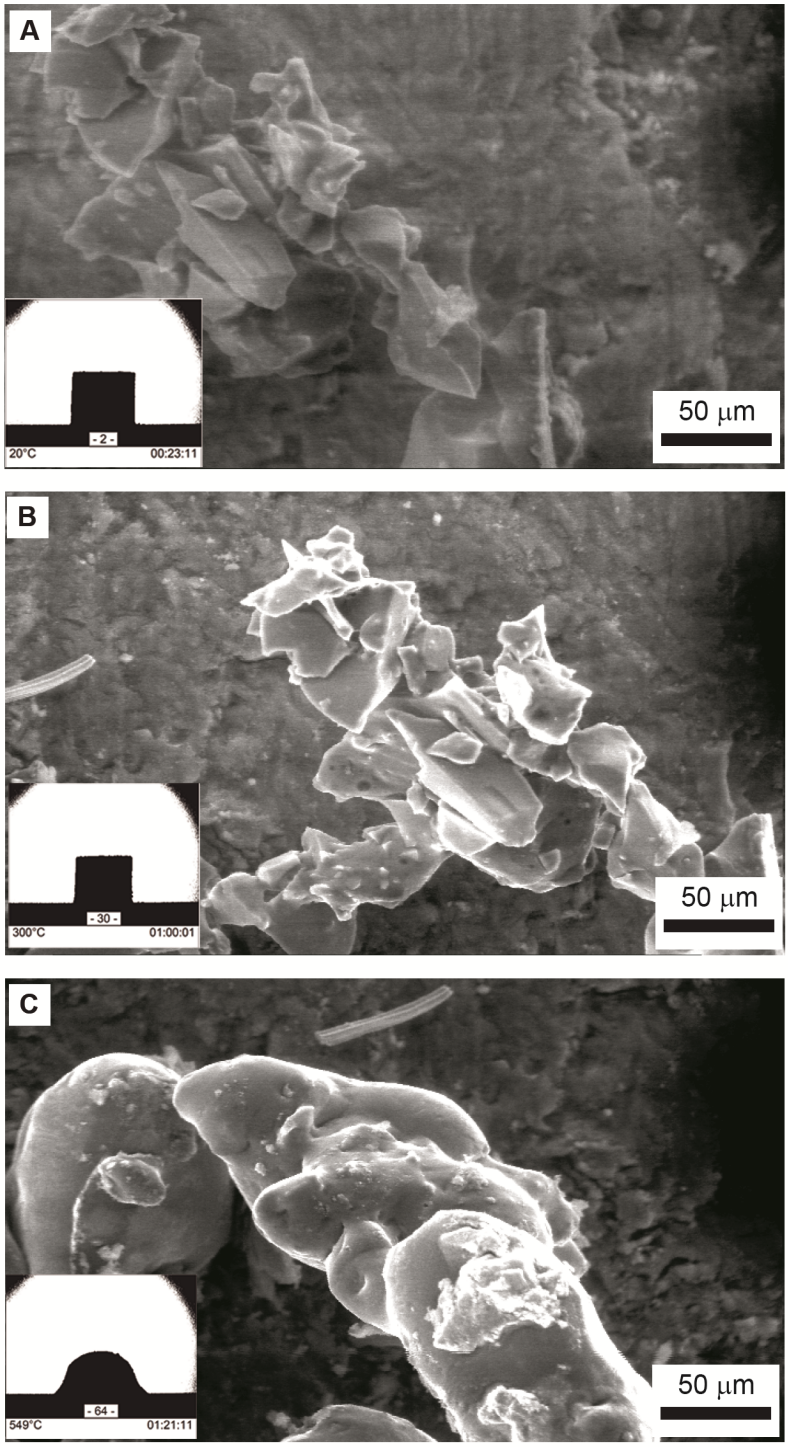

FIGURE 3

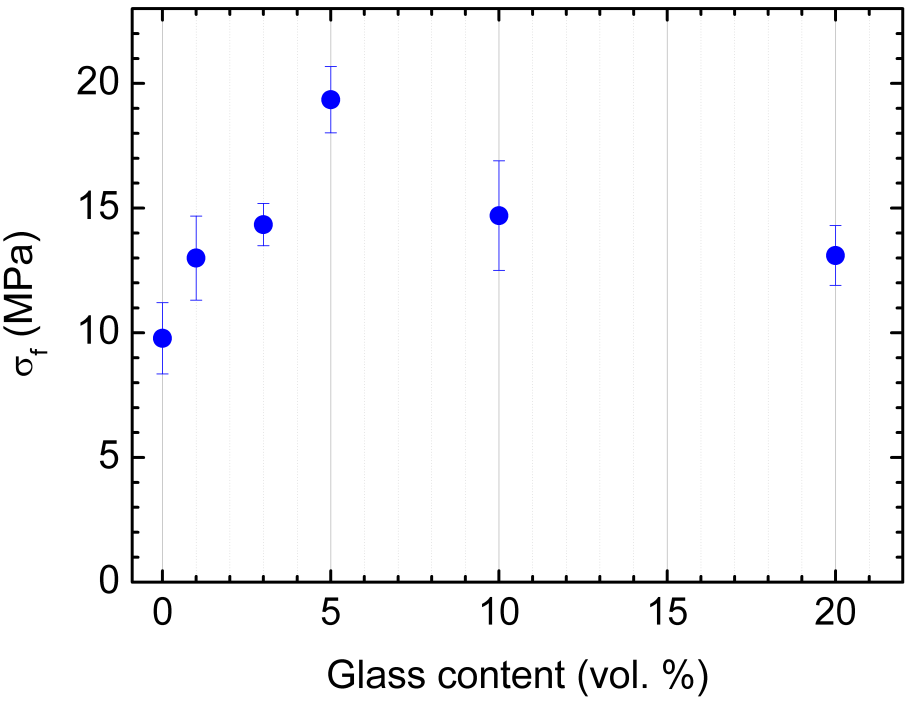

FIGURE 4

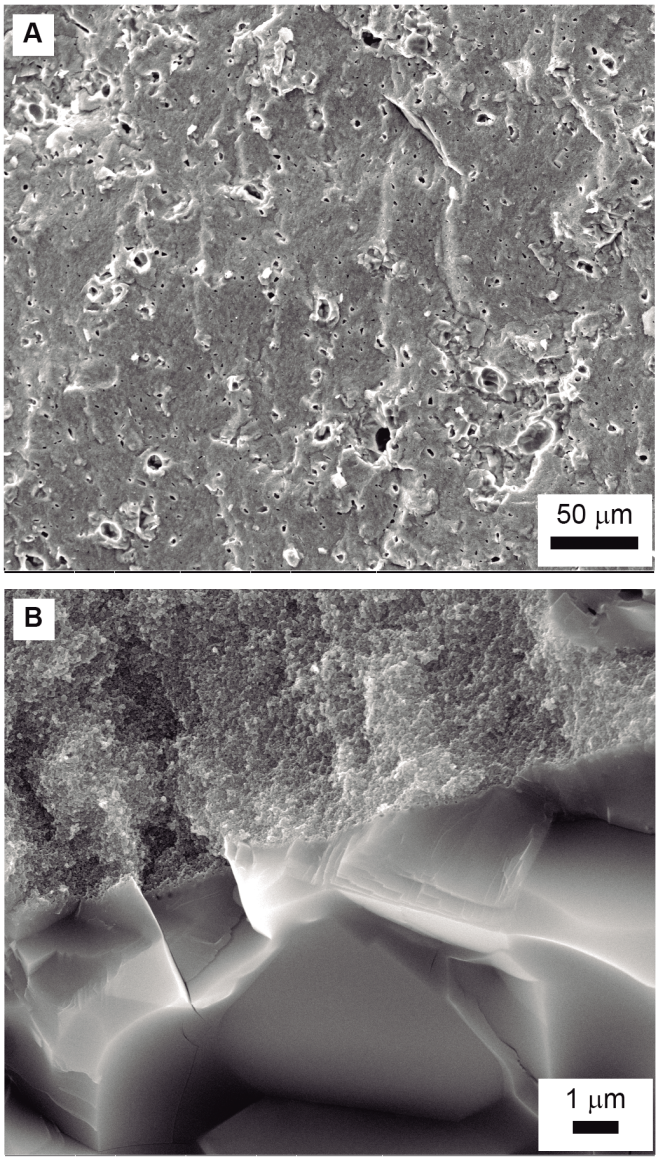

FIGURE 5

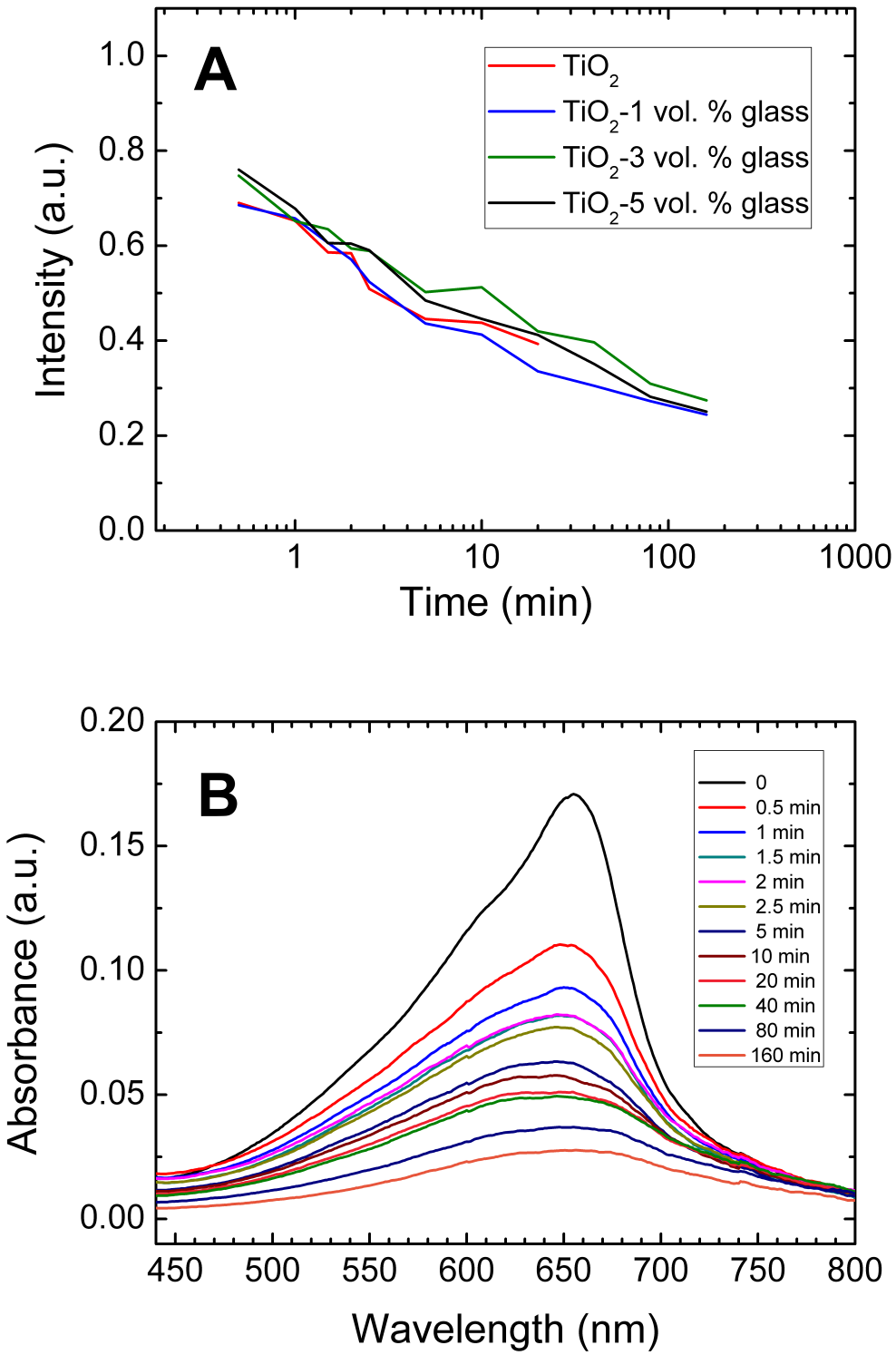
A
TiO2
TiO2-1 vol. % glass
TiO2-3 vol. % glass
TiO2-5 vol. % glass
Intensity (a.u.)
Time (min)
1.0
0.8
0.6
0.4
0.2
0.0
1
10
100
1000
B
0
0.5 min
1 min
1.5 min
2 min
2.5 min
5 min
10 min
20 min
40 min
80 min
160 min
Absorbance (a.u.)
Wavelength (nm)
0.20
0.15
0.10
0.05
0.00
450
500
550
600
650
700
750
800

REFERENCES

[1] J. Schneider, M. Matsuoka, M. Takeuchi, J. Zhang, Y. Horiuchi, M. Anpo, D.W. Bahnemann, Understanding TiO2photocatalysis: Mechanisms and materials, Chem. Rev. 114 (2014) 9919–9986. doi:10.1021/cr5001892.

[2] B.A. van Driel, P.J. Kooyman, K.J. van den Berg, A. Schmidt-Ott, J. Dik, A quick assessment of the photocatalytic activity of TiO2 pigments - From lab to conservation studio!, Microchem. J. 126 (2016) 162–171. doi:10.1016/j.microc.2015.11.048.

[3] M.A. Henderson, A surface science perspective on TiO2 photocatalysis, Surf. Sci. Rep. 66 (2011) 185–297. doi:10.1016/j.surfrep.2011.01.001.

[4] A. Ajmal, I. Majeed, R.N. Malik, H. Idriss, M.A. Nadeem, Principles and mechanisms of photocatalytic dye degradation on TiO 2 based photocatalysts: A comparative overview, RSC Adv. 4 (2014) 37003–37026. doi:10.1039/c4ra06658h.

[5] M.A. Behnajady, N. Modirshahla, M. Shokri, H. Elham, A. Zeininezhad, The effect of particle size and crystal structure of titanium dioxide nanoparticles on the photocatalytic properties, J. Environ. Sci. Heal. - Part A Toxic/Hazardous Subst. Environ. Eng. 43 (2008) 460–467. doi:10.1080/10934520701796267.

[6] U.I. Gaya, A.H. Abdullah, Heterogeneous photocatalytic degradation of organic contaminants over titanium dioxide: A review of fundamentals, progress and problems, J. Photochem. Photobiol. C Photochem. Rev. 9 (2008) 1–12. doi:10.1016/j.jphotochemrev.2007.12.003.

[7] B. Jalvo, M. Faraldos, A. Bahamonde, R. Rosal, Antimicrobial and antibiofilm efficacy of self-cleaning surfaces functionalized by TiO2 photocatalytic nanoparticles against Staphylococcus aureus and Pseudomonas putida, J. Hazard. Mater. 340 (2017) 160–170. doi:10.1016/j.jhazmat.2017.07.005.

[8] B. Jalvo, M. Faraldos, A. Bahamonde, R. Rosal, Antibacterial surfaces prepared by electrospray coating of photocatalytic nanoparticles, Chem. Eng. J. 334 (2018) 1108–1118. doi:10.1016/j.cej.2017.11.057.

[9] P.V. Laxma Reddy, B. Kavitha, P.A. Kumar Reddy, K.H. Kim, TiO2-based photocatalytic disinfection of microbes in aqueous media: A review, Environ. Res. 154 (2017) 296–303. doi:10.1016/j.envres.2017.01.018.

[10] N.A. Mazurkova, Y.E. Spitsyna, N. V. Shikina, Z.R. Ismagilov, S.N. Zagrebel'nyi, E.I. Ryabchikova, Interaction of titanium dioxide nanoparticles with influenza virus, Nanotechnologies Russ. 5 (2010) 417–420. doi:10.1134/S1995078010050174.

[11] M. Cho, H. Chung, W. Choi, J. Yoon, Different inactivation behaviors of MS-2 phage and Escherichia coli in TiO2 photocatalytic disinfection, Appl. Environ. Microbiol. 71 (2005) 270–275. doi:10.1128/AEM.71.1.270-275.2005.

[12] L. Chen, J. Liang, An overview of functional nanoparticles as novel emerging antiviral therapeutic agents, Mater. Sci. Eng. C. 112 (2020) 110924. doi:10.1016/j.msec.2020.110924.

[13] G.D. Venkatasubbu, S. Ramasamy, G.S. Avadhani, L. Palanikumar, J. Kumar, Size-mediated cytotoxicity of nanocrystalline titanium dioxide, pure and zinc-doped hydroxyapatite nanoparticles in human hepatoma cells, J. Nanoparticle Res. 14

(2012). doi:10.1007/s11051-012-0819-3.

[14] X. Valentini, L. Absil, G. Laurent, A. Robbe, S. Laurent, R. Muller, A. Legrand, D. Nonclercq, Toxicity of TiO2 nanoparticles on the NRK52E renal cell line, Mol. Cell. Toxicol. 13 (2017) 419–431. doi:10.1007/s13273-017-0046-1.

[15] J. Hou, L. Wang, C. Wang, S. Zhang, H. Liu, S. Li, X. Wang, Toxicity and mechanisms of action of titanium dioxide nanoparticles in living organisms, J. Environ. Sci. (China). 75 (2019) 40–53. doi:10.1016/j.jes.2018.06.010.

[16] X. Jiang, M. Manawan, T. Feng, R. Qian, T. Zhao, G. Zhou, F. Kong, Q. Wang, S. Dai, J.H. Pan, Anatase and rutile in evonik aeroxide P25: Heterojunctioned or individual nanoparticles?, Catal. Today. 300 (2018) 12–17. doi:10.1016/j.cattod.2017.06.010.

[17] T. Luttrell, S. Halpegamage, J. Tao, A. Kramer, E. Sutter, M. Batzill, Why is anatase a better photocatalyst than rutile? - Model studies on epitaxial TiO2 films, Sci. Rep. 4 (2014). doi:10.1038/srep04043.

[18] J. Varghese, P. Ramachandran, M. Sobocinski, T. Vahera, H. Jantunen, ULTCC Glass Composites Based on Rutile and Anatase with Cofiring at 400 °C for High Frequency Applications, ACS Sustain. Chem. Eng. 7 (2019) 4274–4283. doi:10.1021/acssuschemeng.8b06048.

[19] A.L. Wani, A. Ara, J.A. Usmani, Lead toxicity: A review, Interdiscip. Toxicol. 8 (2015) 55–64. doi:10.1515/intox-2015-0009.

[20] Https://eur-lex.europa.eu/eli/reg/2015/628/oj, EUR-Lex - 32015R0628 - EN - EUR-Lex, Off. J. Eur. Union. (2015) L104/2-L104/5. https://eur-

lex.europa.eu/eli/reg/2015/628/oj (accessed April 21, 2020).

[21] W. Liu, J. Sanz, C. Pecharromán, I. Sobrados, S. Lopez-Esteban, R. Torrecillas, D.-Y. Wang, J.S. Moya, B. Cabal, Synthesis, characterization and applications of low temperature melting glasses belonging to P2O5CaONa2O system, Ceram. Int. 45 (2019) 12234–12242. doi:10.1016/J.CERAMINT.2019.03.133.

[22] A. Smirnov, J.F. Bartolomé, Mechanical properties and fatigue life of ZrO2–Ta composites prepared by hot pressing, J. Eur. Ceram. Soc. 32 (2012) 3899–3904. doi:10.1016/J.JEURCERAMSOC.2012.06.017.

[23] A. Smirnov, J.F. Bartolomé, Microstructure and mechanical properties of ZrO2 ceramics toughened by 5–20vol% Ta metallic particles fabricated by pressureless sintering, Ceram. Int. 40 (2014) 1829–1834. doi:10.1016/j.ceramint.2013.07.084.

[24] D.A.H. Hanaor, C.C. Sorrell, Review of the anatase to rutile phase transformation, J. Mater. Sci. 46 (2011) 855–874. doi:10.1007/s10853-010-5113-0.

[25] A. Markowska-Szczupak, K. Ulfig, A.W. Morawski, The application of titanium dioxide for deactivation of bioparticulates: An overview, Catal. Today. 169 (2011) 249–257. doi:10.1016/j.cattod.2010.11.055.

[26] A. Fujishima, T.N. Rao, D.A. Tryk, Titanium dioxide photocatalysis, J. Photochem. Photobiol. C Photochem. Rev. 1 (2000) 1–21. doi:10.1016/S1389-5567(00)00002-2.

[27] C.R. Tubío, A. Rama, M. Gómez, F. del Río, F. Guitián, A. Gil, 3D-printed

graphene-Al2O3 composites with complex mesoscale architecture, Ceram. Int. 44 (2018) 5760–5767. doi:10.1016/j.ceramint.2017.12.234.

[28] C.R. Tubío, J.A. Nóvoa, J. Martín, F. Guitián, J.R. Salgueiro, A. Gil, Broadband terahertz ZnO photonic crystals fabricated by 3D printing, Ceram. Int. 45 (2019) 6223–6227. doi:10.1016/j.ceramint.2018.12.100.

[29] T. An, K.T. Hwang, J.H. Kim, J. Kim, Extrusion-based 3D direct ink writing of NiZn-ferrite structures with viscoelastic ceramic suspension, Ceram. Int. 46 (2020) 6469–6476. doi:10.1016/j.ceramint.2019.11.127.

[30] I. Capasso, B. Liguori, L. Verdolotti, D. Caputo, M. Lavorgna, E. Tervoort, Process strategy to fabricate a hierarchical porosity gradient in diatomite-based foams by 3D printing, Sci. Rep. 10 (2020). doi:10.1038/s41598-019-55582-0.

[31] J.M. Pappas, X. Dong, Porosity characterization of additively manufactured transparent MgAl2O4 spinel by laser direct deposition, Ceram. Int. 46 (2020) 6745–6755. doi:10.1016/j.ceramint.2019.11.164.